REPORT DOCUMENTATION PAGE

Form Approved
OMB No. 0704-0188

1. AGENCY USE ONLY (Leave Blank)	2. REPORT DATE 22 MAY 1996	3. REPORT TYPE AND DATES COVERED PROFESSIONAL PAPER

4. TITLE AND SUBTITLE

STATUS OF A COMPREHENSIVE VALIDATION OF THE NAVY'S F/A-18A/B/C/D AERODYNAMICS MODEL

5. FUNDING NUMBERS

6. AUTHOR(S)

MICHAEL S. BONNER AND DAVID R. GINGRAS

7. PERFORMING ORGANIZATION NAMES(S) AND ADDRESS(ES)

COMMANDER
NAVAL AIR WARFARE CENTER AIRCRAFT DIVISION
22541 MILLSTONE ROAD
PATUXENT RIVER, MARYLAND 20670-5304

8. PERFORMING ORGANIZATION REPORT NUMBER

9. SPONSORING / MONITORING AGENCY NAME(S) AND ADDRESS(ES)

COMMANDER
NAVAL AIR SYSTEMS COMMAND
1421 JEFFERSON DAVIS HIGHWAY
ARLINGTON, VA 22243

10. SPONSORING / MONITORING AGENCY REPORT NUMBER

11. SUPPLEMENTARY NOTES

12a. DISTRIBUTION / AVAILABILITY STATEMENT

APPROVED FOR PUBLIC RELEASE; DISTRIBUTION UNLIMITED.

12b. DISTRIBUTION CODE

13. ABSTRACT (Maximum 200 words)

A flight test program was designed and flown with two U.S. Navy F/A-18 aircraft and the Naval Air Warfare Center Aircraft Division, Patuxent River, MD to collect data for validation of the Manned Flight Simulator's F/A-18 aerodynamics model. This paper details the flight test program and the processes used to calibrate the flight data for the creation of a truth-data set to be used for the validation as well as source for future updates. The paper presents examples of preliminary aerodynamic coefficient comparisons between model predicted values and values extracted from flight. It also provides a discussion of a coefficient comparison acceptance criteria currently being developed.

14. SUBJECT TERMS
F/A-18; AERODYNAMIC

15. NUMBER OF PAGES
11

16. PRICE CODE

17. SECURITY CLASSIFICATION OF REPORT	18. SECURITY CLASSIFICATION OF THIS PAGE	19. SECURITY CLASSIFICATION OF ABSTRACT	20. LIMITATION OF ABSTRACT
UNCLASSIFIED	UNCLASSIFIED	UNCLASSIFIED	N/A

19960620 112

DTIC QUALITY INSPECTED 1

Encl (5)

STATUS OF A COMPREHENSIVE VALIDATION OF THE NAVY'S F/A-18A/B/C/D AERODYNAMICS MODEL

Michael S. Bonner
Naval Air Warfare Center Aircraft Division
Flight Vehicle Simulation Branch
MS-3, 48140 Standley Rd.
Patuxent River, 20670-5304
(301)342-7601 FAX:(301)342-7607

David R. Gingras[*]
Science Applications International Corporation
Systems Technology Group
44417 Pecan Court, Suite B
California, MD 20619-3272 USA
(301)863-5077 FAX:(301)863-0299

Abstract

A flight test program was designed and flown with two United States Navy F/A-18 aircraft at the Naval Air Warfare Center, Patuxent River, MD to collect data for validation of the Manned Flight Simulator's F/A-18 aerodynamics model. This paper details the flight test program and the processes used to calibrate the flight data for the creation of a truth-data set to be used for the validation as well as source for future updates. The paper presents examples of preliminary aerodynamic coefficient comparisons between model predicted values and values extracted from flight. It also provides a discussion of a coefficient comparison acceptance criteria currently being developed.

Nomenclature

Symbols

C_x	Axial force coefficient.
C_y	Lateral force coefficient
C_z	Normal force coefficient
F	Force, (lbs)
g	Gravity, (32.174 ft/s^2)
I_{xx}	Moment of inertia about X- axis — body frame, (lbs-ft^2)
I_{yy}	Moment of inertia about Y- axis — body frame, (lbs-ft^2)
I_{zz}	Moment of inertia about Z- axis — body frame, (lbs-ft^2)
I_{xy}, I_{xz}, I_{yz}	Products of inertia, (lbs-ft^2)
m	Mass, (slugs).
M	Moment, (ft-lbs)
N	Number of samples
p	Roll rate, (rad/s)
q	Pitch rate, (rad/s)
$\bar{q}$	Dynamic pressure (psf)
r	Process output or yaw rate, (rad/s)
S	Reference planform area, (ft^2)
u	X-axis velocity — body frame, (ft/s)
U	Theil Inequality Coefficient
v	Y-axis velocity — body frame, (ft/s)
V_{True}	Velocity, (ft/s)
w	Z-axis velocity — body frame, (ft/s)
W_c...	Weighting factor
X,Y	Arbitrary parameters
α	Angle of attack, (rad)
β	Angle of sideslip, (rad)
ϕ	Roll angle, (rad)
θ	Pitch angle, (rad)
ψ	Yaw angle, (rad)
ρ	Correlation coefficient
σ	Standard deviation

A_x	Longitudinal acceleration, (ft/s^2)
A_y	Lateral acceleration, (ft/s^2)
A_z	Normal acceleration, (ft/s^2)
b	Wing span, (ft)
c	Mean aerodynamic chord, (ft)
C_D	Drag coefficient
C_l	Rolling moment coefficient.
C_L	Lift coefficient
C_m	Pitch moment coefficient
C_n	Yawing moment coefficient

---

[*] Aerospace Engineer, Member AIAA

1

Subscripts

m   measured
i,j,k Indices.

Superscripts

^   Estimated
~   Derived quantity
—   Mean value

Introduction

The Manned Flight Simulator (MFS) is responsible for providing real-time and non-real-time simulation support for the test and evaluation of naval aircraft[1]. As part of this task, the MFS has maintained high-fidelity 6 degree-of-freedom (DOF) simulations of the F/A-18 A/B/C/D aircraft, including support for several common ordnance loadings. The original F/A-18 A/B simulation was received from McDonnell-Douglas Aerospace (MDA) in 1983 and was adapted to fit the MFS standard simulation architecture known as the Controls Analysis and Simulation Test Loop Environment (CASTLE). Since then, the Navy has made a considerable effort to improve the F/A-18 simulation aerodynamics model using wind-tunnel data, parameter identification (PID), and manual adjustment based on pilot flying qualities assessments[2,3,4,5].

Many components of the F/A-18 aerodynamics model have been compared to wind-tunnel data as well as flight data[3,4,6]. The efforts have served well for the verification, and in some cases validation, of the aerodynamics model at various stages of its development.

The main goal of this effort is to perform a comprehensive evaluation of the F/A-18 aerodynamic model's capability to accurately predict the aerodynamic coefficients using flight data collected from test flights spanning the normal flight envelope as defined in the United States (U.S.) Navy F/A-18 NATOPS flight manual[7]. A secondary goal is to develop a well-documented "truth" data set to be used to evaluate potential modifications to the model.

The diagram in Fig. 1 outlines the process used to validate the F/A-18 aerodynamics model. This paper details each step of the process while providing insight into the problems encountered while analyzing data collected with production aircraft sensors. The paper will also present an example of preliminary aerodynamic coefficient comparisons and results as well as discuss plans for future work.

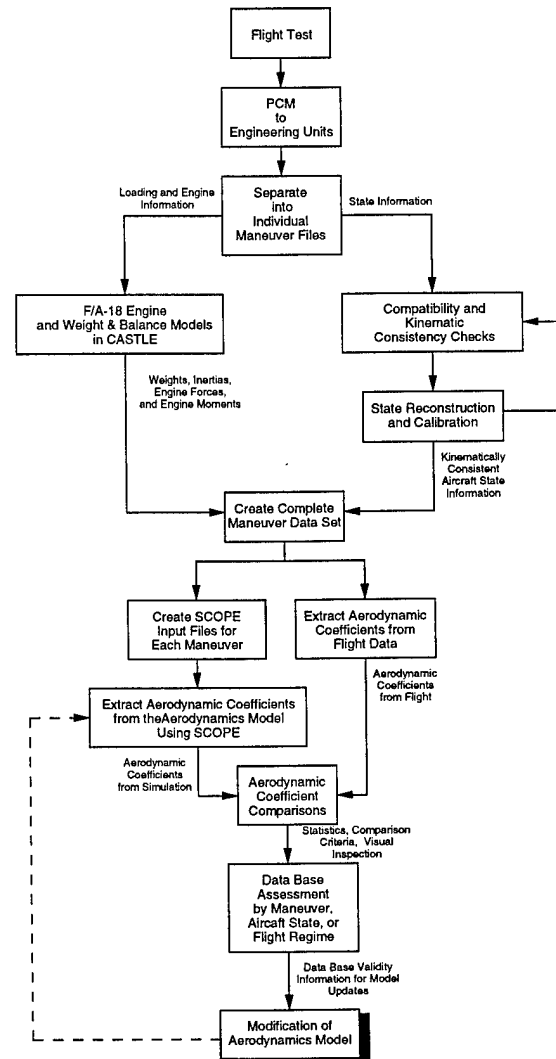Functional Diagram of Aerodynamics Model Validation Data Processing

Fig. 1 Validation process diagram.

Flight Tests

Data from over 2000 individual maneuvers were collected with two aircraft in five different loading configurations during 33 test flights consisting of over 100 hours of flight time using F/A-18A BuNo 161744 (SD-102), a Lot V single-seat aircraft, and F/A-18D BuNo 163986 (SD-113), a Lot XII two-seat aircraft (Fig. 2).

Instrumentation

Both aircraft were equipped with production instrumentation as well as a Quick Installation Data System (QUIDS) package to record variables from the 1553 MUX bus on magnetic tape. Because of time and budget constraints, production aircraft sensors were used
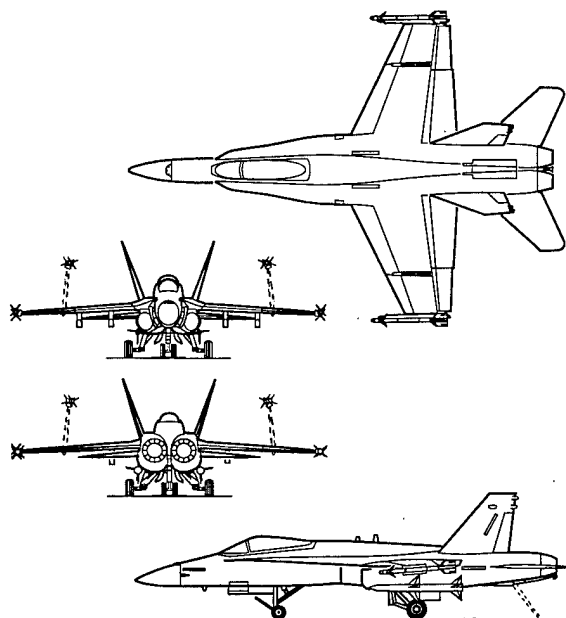
Fig. 2 Four-view diagram of the F/A-18 C.

Fig. 3 F/A-18 test loadings.

to measure all variables with the exception of fuel quantities in SD-102. Fuel sensors were added to SD-102 because they were unavailable on the MUX bus. Multiple redundant variables were recorded for backup and kinematic consistency checking and calibration.

The F/A-18 contains both redundant Flight Control Set (FCS) and strap-down Inertial Navigation Set (INS) angular-rate and linear acceleration sensors. The SD-102 test aircraft contained an ASN-130A INS which uses mechanical angular-rate gyroscopes, while SD-113 contained an ASN-139, which uses ring-laser gyroscopes.

The F/A-18 also has an Air-Data Computer (ADC) that provides the Mission Computer (MC) with ambient and total temperatures, local and true angle of attack, static and impact pressure, mach number, true and indicated airspeed, pressure altitude, and magnetic heading. Information is provided to the ADC by a total-temperature probe, a nose mounted pitot probe, and dual angle-of-attack vanes mounted on the lower fore-body of the fuselage.

Loadings

Data were collected with five of the six basic aircraft loadings. The single-seat F/A-18 was flown in the fighter-escort (FE), fighter-escort with center-line tank (FCL), and interdiction loadings (INT). Because of time constraints only FE and FCL loadings were flown with the two-seat aircraft. Figure 3 contains a diagram detailing each of the loading configurations. Weight and balance information was computed using the MFS F/A-18 simulation weight and balance model. Details
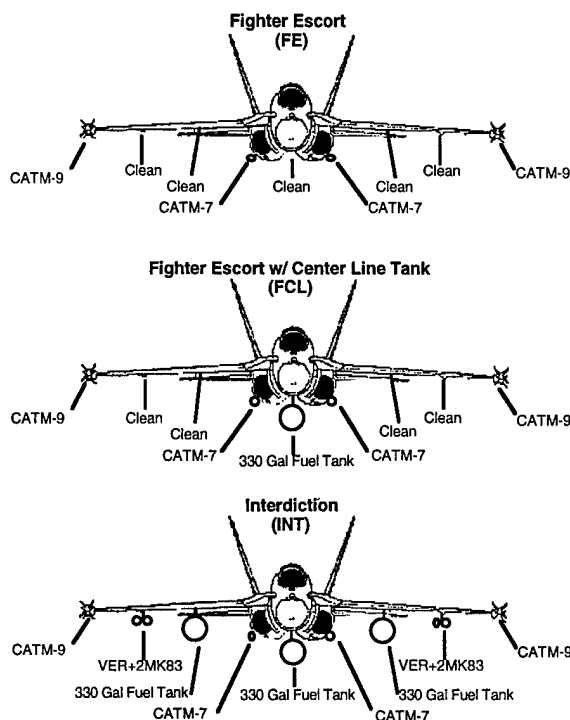
concerning weight and balance information for each loading are presented in Table I.

Test Matrix

The test matrix was designed to cover the standard flight envelope as defined in the F/A-18 Naval Aviation Training and Operational Procedures Manual (NATOPS). Integrated test blocks were flown in level 1G flight conditions for the indicated Mach number. Additional maneuvers were performed in accelerated conditions at 35,000 ft altitude. Powered Approach, full- (PA) and half-flap (PA1/2), data were collected at 6°, 8.1° (on-speed), 10°, and 12° AOA at 5,000 ft altitude. Figure 4 contains a graphic of the single-seat test envelope. The two-seat test envelope is shown in Fig. 5.

Table I contains a break down of the maneuvers flown with the three-axis control augmentation system on (CAS). Additional test points were flown with CAS only in the pitch axis to collect data for future parameter identification efforts. Integrated Test Blocks (ITB) containing maneuvers such as 3211s, various rolls (180°, bank-to-bank, etc.), and steady heading sideslips were designed to stimulate motion in each of the three main axes at each flight condition[8]. Additional maneuvers were flown to gather wind-condition and aircraft performance information.
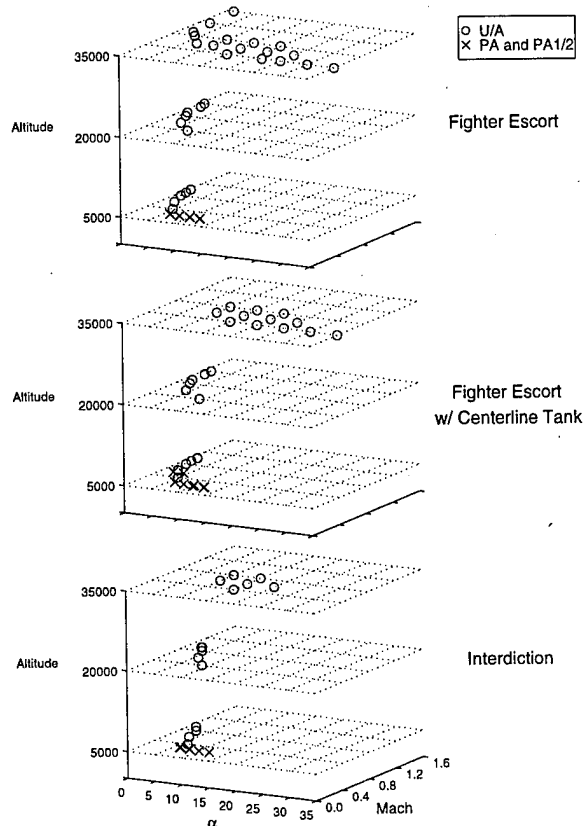
3

Fig. 4 F/A-18 A test envelope.

During test plan development prior to the flight test, many of the ITBs were flown in the MFS F/A-18 real-time simulator by the test pilots. After pre-flying test points, the pilots were able to provide valuable input to the formation of a final flight plan as well as
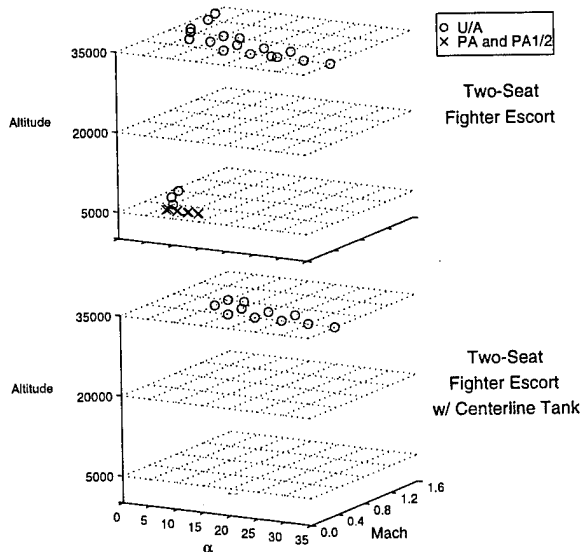

Fig. 5 F/A-18 D test envelope.

Table I. Maneuvers flown and analyzed for the validation effort.

Model	Loading	Maneuvers Flown	Maneuvers Analyzed
A	FE	462	190
	FCL	317	155
	INT	261	110
D	FE	320	134
	FCL	75	51
	TOTAL	1435	640

take note of potentially hazardous areas of the test matrix. This also provided pilot training for some of the non-standard maneuvers used in this project.

Validation Data Set

One of the main objectives in creating the validation data set was to establish a set of calibrated, kinematically consistent data. The flight data were analyzed for consistency among redundant sources, then were verified for kinematic consistency. In cases where data were not consistent, calibrations were applied and the data rechecked for consistency. The following sections present results of this process.

Redundant Measurement Consistency Check

A redundant-measurement flight-data consistency check was performed to assess the quality of the measured flight data. During this process, redundant variables recorded by the INS, the Flight Control Electronics Set (FCS), and the ADC sensors were compared to one another. Redundant sensors were available for angular rates and linear accelerations.

FCS/INS Sensors

Measurements from FCS and INS sensors were consistent with one another in most cases for both SD-102 and SD-113. For both aircraft, dynamic matching between FCS and INS angular-rate sensors was excellent. Figure 6 contains a typical comparison of FCS angular rates to the INS wide-band rates for a pitch 3211 maneuver performed by SD-102.

During data reduction linear accelerations measured by the FCS and INS had been recomputed at the aircraft center of gravity using sensor locations noted in weight and balance reports. A problem was seen in comparisons of lateral acceleration signals during high roll rate maneuvers performed by both aircraft. Large discrepancies, such as 6 ft/sec^2 errors in lateral acceleration during a 200+ deg/sec roll rate, were seen in the single-seat data. Using parameter identification techniques [9], an error in the INS lateral sensor position on the order of 0.5 in was estimated. Further research
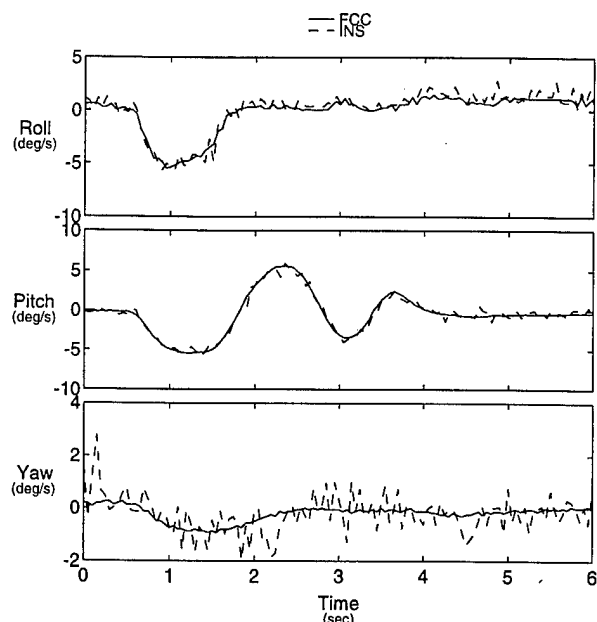
Fig. 6 Wide-band INS angular rate measurements compared to FCS rate measurements.

lead to a McDonnell Douglas Aerospace internal memo noting a "center of navigation" position for the INS that validated the position error estimate[10].

Comparisons between INS and FCS signals also revealed a time delay between the two for both aircraft. Wide-band INS signals were in sync with FCS quantities, while narrow-band INS signals were delayed by approximately 0.1 to 0.2 seconds (Fig. 7). The dynamics represented in the signals were almost identical.

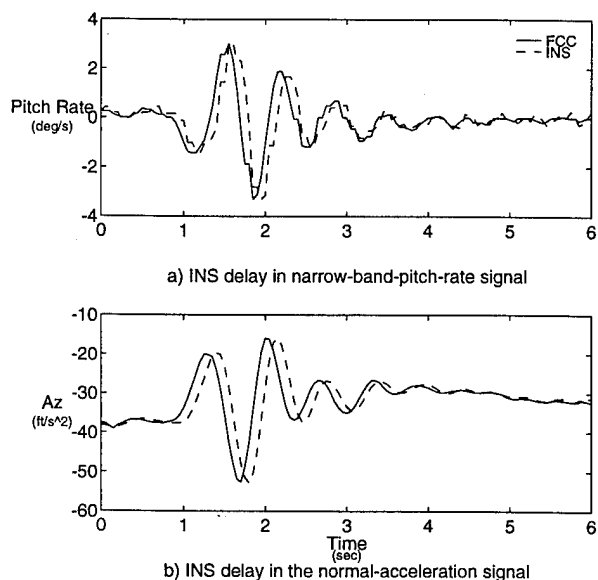A decision was made to use INS signals for several

reasons. First, during the analysis of SD-102 data it was found that FCS rate gyros would sometimes stop updating for one frame during high-rate maneuvers. This phenomenon was seen randomly throughout maneuvers and could not be correlated with any variables. Next, only normal and lateral accelerations were available from the FCS sensors, therefore the INS axial accelerations *had* to be used. And last, delays of the same magnitude as those of the INS narrow-band signal were found in the recorded control surface positions[11]. The use of aircraft information with inconsistent time tags as input to the aerodynamics model to extract aerodynamic coefficients can lead to erroneous coefficient comparisons.

ADC/INS Sensors

Several comparisons were made between redundant angle of attack measurements for a variety of test points. The majority of the comparisons matched dynamically, but were biased from each other (Fig. 8a). At angles of attack exceeding 15°, consistency between the INS and ADC was lost (Fig. 8b).

Flight Data Kinematic Consistency

To ensure the compatibility of the measured flight data, a kinematic consistency analysis was performed. The objective of the analysis was to ensure the measured aircraft state was consistent with its corresponding state reconstructed by integrating the equations of motion.

The equations used in the analysis were the six-degree-of-freedom-kinematic equations of motion

a) INS delay in narrow-band-pitch-rate signal

b) INS delay in the normal-acceleration signal

Fig. 7 INS and FCS measurement comparisons showing a delay in INS signals.

a) Low-angle-of-attack discrepancies between ADC and INS

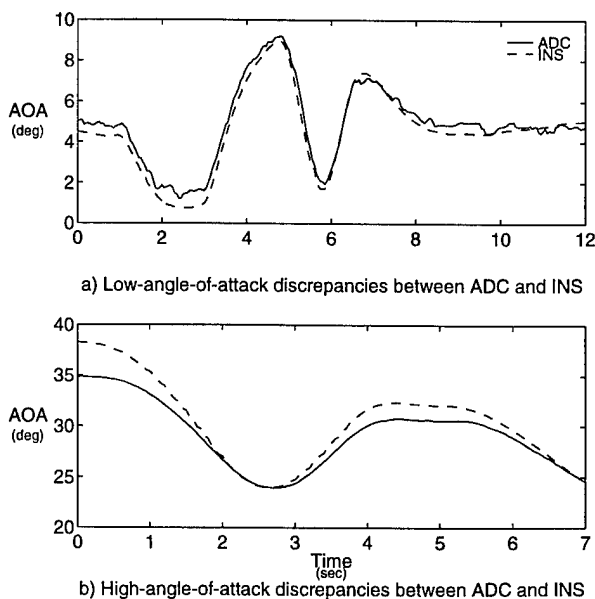b) High-angle-of-attack discrepancies between ADC and INS

Fig. 8 High- and low-angle-of-attack ADC and INS angle of attack comparisons.

5

assuming a non-rotating earth and constant winds[12,9,13]. (equation set 1). Aircraft velocity components and attitude were computed using a second-order-open Adams-Bashforth integration algorithm with INS measured linear accelerations and angular rates as inputs.

$$\hat{u}_i = A_{x_i} - g\sin\hat{\theta}_i - q_i\hat{w}_i + r_i\hat{v}_i$$

$$\hat{v}_i = A_{y_i} + g\sin\hat{\phi}_i\cos\hat{\theta}_i - r_i\hat{u}_i + p_i\hat{w}_i$$

$$\hat{w}_i = A_{z_i} + g\cos\hat{\phi}_i\cos\hat{\theta}_i - p_i\hat{v}_i + q_i\hat{u}_i$$

$$\hat{\psi}_i = (q_i\sin\hat{\phi}_i + r_i\cos\hat{\phi}_i)/\cos\hat{\theta}_i \qquad (1)$$

$$\hat{\theta}_i = q_i\cos\hat{\phi}_i - r_i\sin\hat{\phi}_i$$

$$\hat{\phi}_i = p_i + (q_i\sin\hat{\phi}_i + r_i\cos\hat{\phi}_i)\tan\hat{\theta}_i$$

$$\hat{h}_i = \hat{u}_i\sin\hat{\theta}_i - \hat{v}_i\sin\hat{\phi}_i\cos\hat{\theta}_i - \hat{w}_i\cos\hat{\phi}_i\cos\hat{\theta}_i$$

Angular accelerations used in the equations were determined using a second-order-central-difference numerical algorithm.

The chosen observation variables included the aircraft attitude angles, $\hat{\phi}$, $\hat{\theta}$, $\hat{\psi}$, h, and the aircraft wind-relative velocity and flow angles, $\hat{V}_{true}$, $\hat{\alpha}$, $\hat{\beta}$ (equation set 2).

$$\hat{V}_{true} = \sqrt{\hat{u}^2 + \hat{v}^2 + \hat{w}^2}$$

$$\hat{\alpha} = \tan^{-1}\left(\frac{\hat{w}}{\hat{u}}\right) \qquad (2)$$

$$\hat{\beta} = \sin^{-1}\left(\frac{\hat{v}}{\hat{V}}\right)$$

Preliminary results showed very consistent aircraft attitude measurements from the INS, but revealed inconsistencies in the ADC velocity and angle-of-attack measurements. Airspeed and angle of attack data quality degraded as angles of attack increased above 15° for Mach numbers less than 0.6. An example of this is shown in data from a 50° AOA push over in Fig. 9. This inconsistency was due to the excessive local angles of attack in the vicinity of the fuselage mounted probes. The production angle-of-attack probes in the F/A-18 are mechanically limited at 56° local angle of attack. This corresponds to approximately 35° true angle of attack, therefore angle-of-attack information above 35° true was lost. Inconsistencies in true airspeed were also found at Mach numbers greater than 0.6 above 10° angle of attack. Analyses of the ADC true velocity signals indicated decreases in airspeed which were not consistent with angle of attack or measured accelerations (Fig. 10).
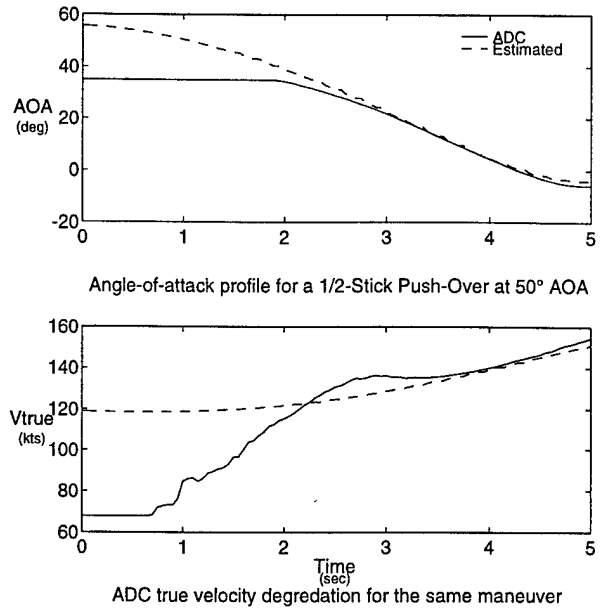

Angle-of-attack profile for a 1/2-Stick Push-Over at 50° AOA

ADC true velocity degredation for the same maneuver

Fig. 9 Production angle-of-attack sensor probe limitations and ADC true velocity degradations at high angles of attack.

Flight Data Calibration and Reconstruction

The main objective in the calibration of the flight data was to create kinematically consistent data by correcting or reconstructing data that may have been corrupted by measurement error. Calibrations and reconstructions were developed by using redundant sensors, enforcing kinematic consistency in the data, and deriving calibration information from alternate data sets.

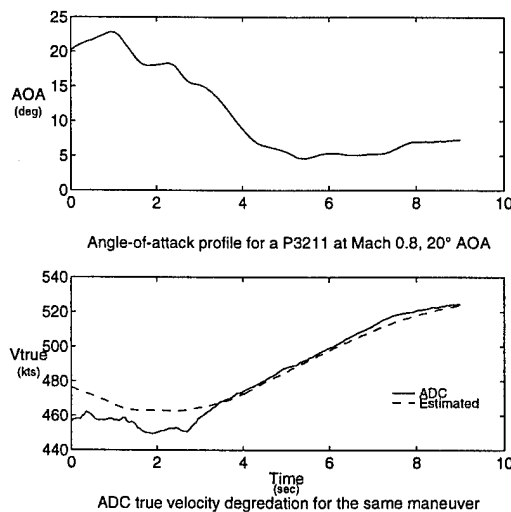

Angle-of-attack profile for a P3211 at Mach 0.8, 20° AOA

ADC true velocity degredation for the same maneuver

Fig. 10 Example of ADC reported true velocity inconsistencies for Mach numbers greater than 0.6 at moderate angles of attack.

6

True Velocity and Angle of Attack

Air data for high-angle-of-attack maneuvers were reconstructed by combining the short-term accuracy of the INS with the long-term accuracy of the ADC. This approach was a compromise between using ADC data that were poor at high angles of attack and using INS data that seemed to be biased at low angles of attack. The air-data reconstruction was based on the assumptions of constant winds, negligible vertical wind component, and accurate MC reported wind measurements below 25° AOA. Wind-relative aircraft velocities were computed in the inertial frame of reference by subtracting mission computer reported winds from INS report inertial velocities. The wind relative velocities were then transferred from the inertial frame to the body reference frame where they were used to compute true airspeed and angle of attack.

This method was applied to all test points regardless of the flight condition to maintain a common data source among all air data. An example of the results from the air data reconstruction is presented in Fig. 10.

Angle of Sideslip

Preliminary comparisons of estimated angle of sideslip and INS sideslip indicated drift and bias errors. The F/A-18 has no production sensor to directly measure angle of sideslip (AOS). The variable is calculated by the mission computer using fixed wind estimates as illustrated in Fig. 11. Small changes in atmospheric conditions can lead to sideslip bias and drift errors. To maintain reasonable sideslip measurements, the sideslip signal was initialized before each maneuver or set of maneuvers. These resets were performed by the pilot initiating a HUD reject 2. This action caused the MC to re-calculate the wind estimates assuming zero angle of sideslip. These estimates were frozen for the computation of sideslip.

While initiating a HUD reject 2 the pilot was to maintain steady, wings level, 1g trim flight, without sideslip for at least 10 seconds. Given that neither of the test aircraft were equipped with a sideslip indicator, such as a yaw string or chin vane, the pilot was left to determine when the required condition was met. Human beings, by nature, are unreliable measurement devices[14], therefore random bias errors were introduced into sideslip signal.

The sideslip bias errors were particularly apparent in several cases where preliminary comparisons of simulation predicted lateral-directional coefficients to reconstructed coefficients showed large constant biases which were not consistent with the aircraft state and control surface positions. Small biases were applied to
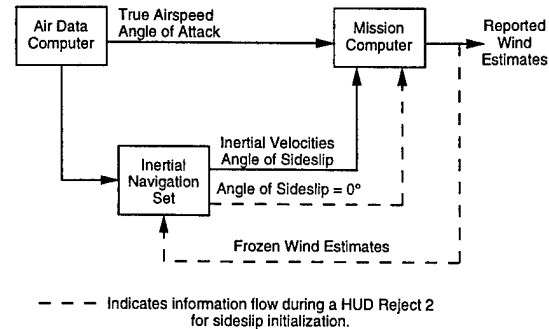

- - - Indicates information flow during a HUD Reject 2 for sideslip initialization.

**Fig. 11** Functional diagram of mission computer angle of sideslip determination

the AOS signal used to drive the simulation, thus improving comparisons of trim values of coefficient comparisons (Fig. 12). Further evidence of angle-of-sideslip biases can be seen by the scatter of circle symbols in Fig 13. The figure contains a plot of INS estimated sideslip for two-seat FE maneuvers against lateral acceleration during the initial trim portion of each maneuver. During this portion of the maneuvers, a linear relationship between sideslip and lateral acceleration was expected.

Several different methods were used in the attempt to calibrate angle of sideslip data. Among them were traditional parameter identification techniques[9], where attempts were made to identify biases in sideslip using a maximum likelihood scheme. A second attempt involved using differential angle-of-attack signals to compute sideslip[11]. Results from this method showed no overall improvement.

The calibration technique which yielded the best
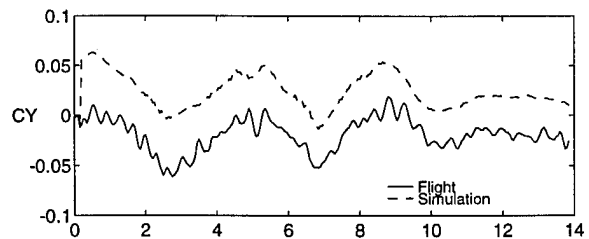
CY from flight compared to simulation predicted CY using raw beta.
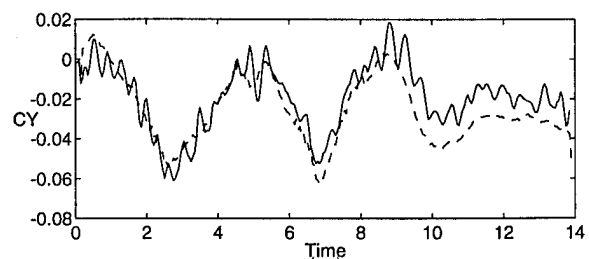
The same comparison with simulation predicted CY using a 1.95 deg bias in beta.

Fig. 12 Side force coefficient comparison showing result of sideslip bias.
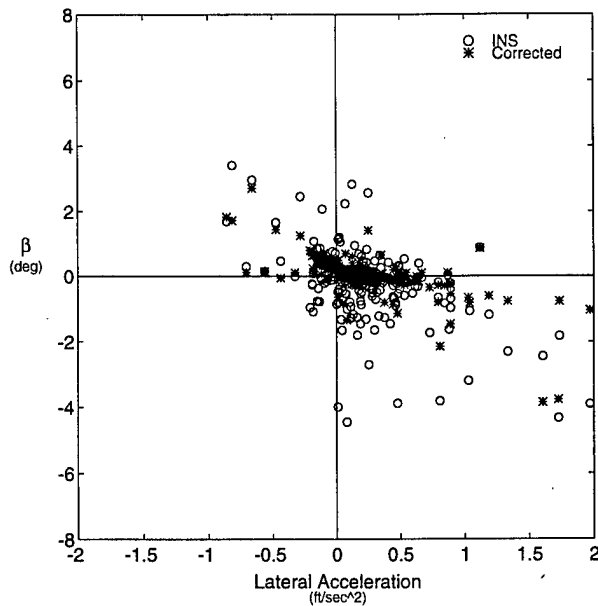
7

Fig. 13 Scatter plot of sideslip angle versus lateral acceleration during trim showing results of the side slip calibration.

results was rather unconventional. An assumption was made that the F/A-18 aerodynamic model accurately predicted lateral-direction coefficients during steady-state, unaccelerated trim conditions. The F/A-18 aerodynamic model inputs were overridden with kinematically consistent aircraft state information (including INS estimated sideslip angle) and measured control surface deflections. Values of C_l, C_n, and C_Y were predicted by the F/A-18 aerodynamics model using an analysis tool called Simulation Checking using an Optimal Prediction Evaluation (SCOPE). These coefficients were compared with corresponding coefficients extracted from flight data for the trim portion of each maneuver. Differences between the coefficients similar to the example shown in Fig. 12, were assumed to be a result of sideslip. Next, using the linear model extraction (LME) tool in CASTLE, values of $C_{l\beta}$, $C_{n\beta}$, and $C_{Y\beta}$ were computed for each data ITB trim condition. Sideslip corrections were determined by combining the contribution of each coefficient comparison and LME derivative using a weighted average as defined in equation set (3).

$$\Delta\beta = W_{C_Y}\Delta\beta_{C_Y} + W_{C_l}\Delta\beta_{C_l} + W_{C_n}\Delta\beta_{C_n}$$

Where Wc_Y, $\Delta\beta c_Y$, Wc_l, $\Delta\beta c_l$, Wc_n and $\Delta\beta c_n$ were determined in the following fashion.

$$W_{C_Y} = \frac{C_{Y_\beta}}{C_{Y_\beta} + C_{l_\beta} + C_{n_\beta}} \tag{3}$$

$$\Delta\beta_{C_Y} = \frac{\Delta C_Y}{C_{Y_\beta}}$$

This process resulted in considerable corrections in sideslip for many maneuvers, but was not effective for maneuvers where trim data were missing. Figure 13 contains a plot of two-seat FE angle of sideslip values versus lateral acceleration during trim for corrected sideslip values (star-shaped symbols) in addition to uncorrected values (circle-shaped symbols). It is easy to notice the improvement in angle-of-sideslip values especially in the region where the aircraft was experiencing little or no lateral acceleration.

The complete calibrated observation parameter set was compared to estimated quantities computed using equation set (1) and (2). Figure 14 presents an example of kinematic data consistency. In general kinematic consistency was very good among the data. Some drift was encountered in several of the estimated observation parameters V_{True}, α, β, ϕ, θ, and ψ. Figure 14 also contains a statistical measure of the quality of the comparison called the Theil inequality coefficient[15], equation set (4). This parameter is the
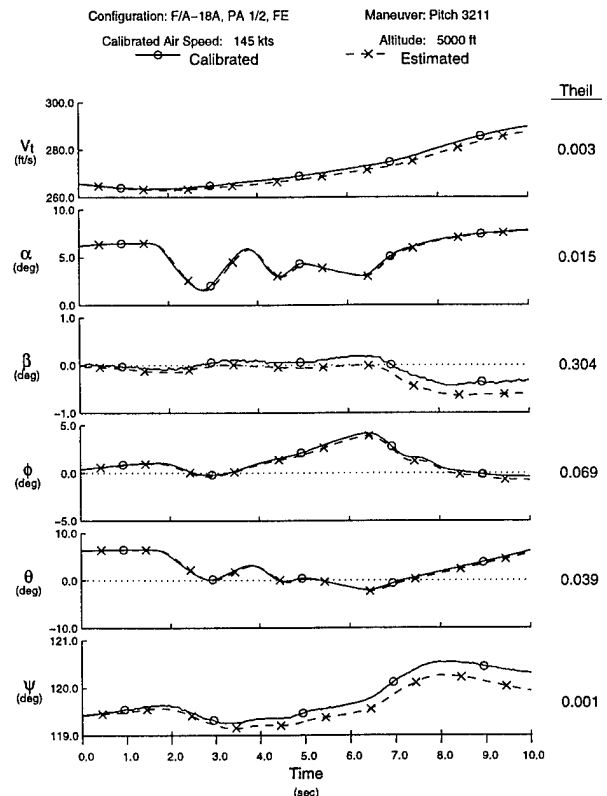

Fig. 14 Example of kinematic consistency.

root mean squared (RMS) error normalized by the sum of the RMS values of the signals being compared. The coefficient ranges from 0, where there are no differences between the two signals, to 1, where the RMS error between the two signals is equal to the sum of the RMS of the two signals.

$$U = \frac{\sqrt{\frac{1}{N}\sum_{i=1}^{N}\left(Y_i - \hat{Y}_i\right)^2}}{\sqrt{\frac{1}{N}\sum_{i=1}^{N}Y_i^2} + \sqrt{\frac{1}{N}\sum_{i=1}^{N}\hat{Y}_i^2}} \tag{4}$$

In addition to the Theil coefficient, error proportions were computed for each maneuver (equation set 5).

$$U_{Bias} = \frac{\left(\overline{Y} - \overline{\hat{Y}}\right)^2}{\frac{1}{N}\sum_{i=1}^{N}\left(Y_i - \hat{Y}_i\right)^2}$$

$$U_{Var} = \frac{\left(\sigma - \hat{\sigma}\right)^2}{\frac{1}{N}\sum_{i=1}^{N}\left(Y_i - \hat{Y}_i\right)^2} \tag{5}$$

$$U_{Cov} = \frac{\left(2(1-\rho)\sigma\hat{\sigma}\right)^2}{\frac{1}{N}\sum_{i=1}^{N}\left(Y_i - \hat{Y}_i\right)^2}$$

where

$$\overline{Y} = \frac{1}{N}\sum_{i=1}^{N}Y_i$$

$$\sigma = \sqrt{\frac{1}{N}\sum_{i=1}^{N}\left(Y_i - \overline{Y}\right)^2}$$

$$\rho = \frac{\frac{1}{N}\sum_{i=1}^{N}\left(Y_i - \overline{Y}\right)\left(\hat{Y}_i - \overline{\hat{Y}}\right)}{\sigma\hat{\sigma}}$$

These statistics, ranging between 0 and 1, indicate sources of differences between two signals. Large values of the covariance proportion indicated differences due to uncorrelated factors such as noise. Large variance proportion values generally indicated scaling errors. Large bias proportion values indicated drift errors. Plots of Theil statistics versus angle of attack and Mach aided the engineers in assessing data quality for the entire 640 maneuvers.

Weight, Balance and Thrust Reconstruction

Prior to the aerodynamic coefficient reconstruction, SCOPE was used to drive the F/A-18 simulation to extract weight, inertial, and center of gravity location predictions from the weight and balance model. Baseline aircraft weights and longitudinal center of gravity (CG) positions were taken from actual measurements of the instrumented test articles performed prior to execution of the flight test program. Fuel-tank quantities were measured during the test and used in the weight and balance model. The simulation model was successfully validated with aircraft weight and balance information from a manufacturer's weight and balance report[16] as well as preflight weight and balance measurements. A detailed uncertainty analysis performed for the data reduction process indicated that fuel weight measurement errors had negligible effects on data reduction results.

Because of time and budget constraints, the test articles' engines were not thoroughly instrumented and calibrated. Thrust estimates were extracted from the F/A-18 simulation engine model for each maneuver condition and throttle setting. The engine model consisted of steady-state engine performance data derived from a non-real-time cycle deck. Static values of net thrust, fuel flow, and related engine operating variables were determined via table lookup based on altitude, ambient temperature, Mach, and throttle position. Second-order filters were used to model dynamic engine response.

Aerodynamic Data Reconstruction

Aerodynamic coefficients were reconstructed from the calibrated data. Rates and accelerations were used with the aircraft mass and inertia characteristics to estimate the total forces and moments acting on the aircraft. From them, forces and moments due to thrust were subtracted, yielding aerodynamic contributions. The aerodynamic forces and moments were non-dimensionalized to provide the aerodynamic coefficients of the aircraft. The longitudinal coefficients were transferred from the body axis to the stability axis and all moment coefficient reference points were transferred from the actual center of gravity to the reference location at 25% mean aerodynamic chord for comparison with the simulation. See equation set (6).

$$C_x = \frac{m}{\bar{q}S}\left(F_x - F_{x_{Eng}}\right)$$

$$C_y = \frac{m}{\bar{q}S}\left(F_y - F_{y_{Eng}}\right)$$

$$C_z = \frac{m}{\bar{q}S}\left(F_z - F_{z_{Eng}}\right)$$

$$C_l = \frac{m}{\bar{q}Sb}\left(M_x - M_{x_{Eng}} - F_y \Delta z_{cg} + F_z \Delta y_{cg}\right)$$

$$C_m = \frac{m}{\bar{q}S\bar{c}}\left(M_y - M_{y_{Eng}} + F_x \Delta z_{cg} - F_z \Delta x_{cg}\right)$$

$$C_n = \frac{m}{\bar{q}Sb}\left(M_z - M_{z_{Eng}} - F_x \Delta y_{cg} + F_y \Delta x_{cg}\right)$$

(6)

with

$$C_L = C_x \sin\alpha - C_z \cos\alpha$$

$$C_D = -C_x \cos\alpha - C_z \sin\alpha$$

where

$$F_X = mA_x$$
$$F_Y = mA_y$$
$$F_Z = mA_z$$

$$M_x = \dot{p}I_{xx} - \dot{q}I_{xy} - \dot{r}I_{xz} + qr\left(I_{zz} - I_{yy}\right) + \left(r^2 - q^2\right)I_{yz} - pqI_{xz} + rpI_{xy}$$

$$M_y = -\dot{p}I_{xy} + \dot{q}I_{yy} - \dot{r}I_{yz} + rp\left(I_{xx} - I_{zz}\right) + \left(p^2 - r^2\right)I_{xz} - qrI_{xy} + pqI_{yz}$$

$$M_z = -\dot{p}I_{xz} - \dot{q}I_{yz} + \dot{r}I_{zz} + pq\left(I_{yy} - I_{xx}\right) + \left(q^2 - p^2\right)I_{xy} - rpI_{yz} + qrI_{xz}$$

Aerodynamic Coefficient Comparisons

The goal of the first phase of the F/A-18 aerodynamics database validation is to identify areas of the database that need improvement. With the vast amount of data collected for the validation, individual aerodynamic coefficient checks for each maneuver became time consuming and subjective. An acceptance criteria is being developed for such an analysis. The objective in developing the criteria is to create a standard definition for "good" and "bad" coefficient comparisons. Some studies have been conducted using a rating system based on the Theil coefficients, but have not yielded promising results. The study is on going.

Several preliminary analyses have been performed using the truth data set. Aerodynamic coefficients were extracted from the Navy's version 3.2 aerodynamics model using SCOPE. Figure 15 illustrates the coefficient comparison process using SCOPE.

One analysis investigated the aerodynamics model's fidelity at high roll rates during maneuvers at varying angles of attack. Figure 16 contains an example comparison of lateral and directional coefficients for a two-seat fighter escort high-roll-rate maneuver. The comparison reveals simulation over predictions of C_y and C_n as well as reasonable, but slight, under-

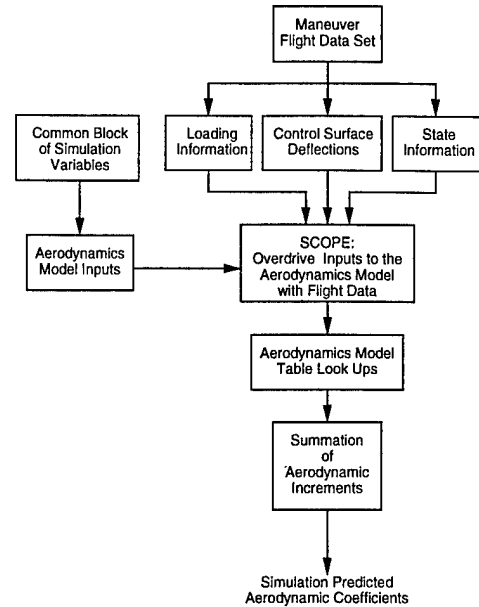Functional Diagram of Aerodynamic Coefficient Extraction Using SCOPE

Fig. 15 Functional diagram of aerodynamic coefficient extraction from the aerodynamics model using SCOPE.

predictions of Cl. Results such as these have lead to an in-depth study into the cause of the discrepancies. Results of the study suggested improvements to the model using dynamic modeling techniques[6].

Summary and Conclusions

An aerodynamics model validation and baseline data set was created using data collected from two production F/A-18 aircraft. Particular care needed to be taken in the interpretation of the multiple production data sources available, for example the direct use of the sideslip angle as provided by the INS may have lead to misinterpretations during validation studies. The processes used to reconstruct and calibrate the data would have been facilitated by the addition of several sensors such as sideslip and a wide-range angle of attack probe. In general, the data are sufficient for validation purposes. Modifications to the angle-of-sideslip calibrations may be in order as investigations into a more elegant methods of bias determination continue.

The complete comprehensive validation of the F/A-18 aerodynamics model is on-going as is work to develop an acceptance criteria for aerodynamic coefficient comparisons.
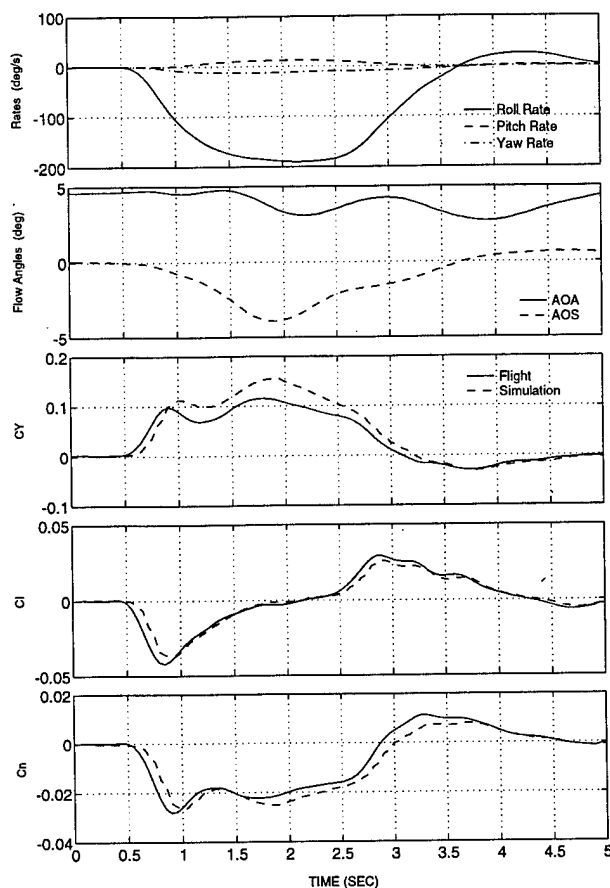
American Institute of Aeronautics and Astronautics

Fig. 16 Lateral-directional coefficient comparison of a two-seat fighter escort high-rate roll maneuver.

References

[1] Burton, R. A., Miller, C. C., and Mills, R E., "Manned Flight Simulator and the Impact on Navy Weapons Systems Acquisition," AIAA-94-3420-CP, August 1994.

[2] Fitzgerald, T.R., et al, "Improvements to the Naval Air Warfare Center Aircraft Division's F/A-18 Subsonic Aerodynamics Model", AIAA-94-3400 Flight Simulation Technologies Conference in Scottsdale, AZ, 1-3 August 1994.

[3] Hess, Robert A., "Subsonic F/A-18A and F/A-18B (TF-18A) Aerodynamics Identified from Flight Test Data", SCT 4522-220-1, July 1987.

[4] Hess, Robert A., "Development and Evaluation of a High-Fidelity F-18 Aerodynamic Model in a Unified Format"; SCT 6007-070-1, October 1989.

[5] O'Connor, Cornelius, "NATC F-18A/B Aerodynamic Math Model Modifications Incorporated during the Phase II Model Unification Effort"; BAR 90-13, September 1990.

[6] Ralston, J. N. et al, "Evaluation of the NAWCAD F/A-18 C/D Simulation Including Data Base

Coverage and Dynamic Data Implementation Techniques," Bihrle Applied Research report number BAR 95-9, December 95.

[7] "NATOPS Flight Manual: Navy Model F/A-18A/B/C/D"; A1-F18AC-NFM-000, 15 January 1991; change 5 — 15 August 1993.

[8] Naval Air Warfare Center Aircraft Division Flight Test and Engineering Group Project Test Plan, " F/A-18 Simulation Validation and Verification Flight Test Program," August 1993.

[9] Klein, V., and Morgan, D., "Estimation of Bias Errors in Measured Airplane Responses Using Maximum Likelihood Method," NASA TM-89059, Jan. 1987.

[10] Pulley C., McDonnell Douglas Aerospace engineer, personal communication regarding informal internal McDonnell Aircraft Company memo titled "GPS Lever Arm Compensation," dated 3 Jan 1992, Fall 1994.

[11] Gingras, D. R., "Validation Documentation," SAIC Report No. 01-1393-3970-B003, March 1996.

[12] Maine, R.E, and Iliff, K.W., "Application of Parameter Estimation to Aircraft Stability and Control," NASA RP-1168, June 1986.

[13] Weiss, S. et al, "System Identification for X-31A Project Support — Lessons Learned so Far—", AGARD FMP Symposium "Flight Testing", Paper No. 14, Chania, Crete, Greece, 11-14 May 1992.

[14] Pepitone,D.D., Shively,R.J., and Bortolussi, M.R., "Pilot-Work-Load Prediction," Paper No. 871771, 6th SAE ABET Conference Long Beach, CA, 1988.

[15] Pindyck, R. S. and Rubinfield, D. L., *Econometric Models and Economic Forecasts Third Edition*, McGraw Hill, New Yaork, NY, 1991.

[16] West, G.R., "Actual Weight and Balance Report for Model F/A-18C Airplane Serial No.163985," MDC B1871, McDonnell Aircraft Company, St Louis, MO, Oct 1989.